Transition-State Analysis of a V_{max} Mutant of AMP Nucleosidase by the Application of Heavy-Atom Kinetic Isotope Effects†

David W. Parkin,‡ Frank Mentch,§ Grace A. Banks,‡ Benjamin A. Horenstein, and Vern L. Schramm*
Department of Biochemistry, Albert Einstein College of Medicine, 1300 Morris Park Avenue, Bronx, New York 10461
Received September 21, 1990; Revised Manuscript Received December 31, 1990

ABSTRACT: The transition state of the V_{max} mutant of AMP nucleosidase from *Azotobacter vinelandii* [Leung, H. B., & Schramm, V. L. (1981) *J. Biol. Chem. 256*, 12823-12829] has been characterized by heavy-atom kinetic isotope effects in the presence and absence of MgATP, the allosteric activator. The enzyme catalyzes hydrolysis of the N-glycosidic bond of AMP at approximately 2% of the rate of the normal enzyme with only minor changes in the K_m for substrate, the activation constant for MgATP, and the K_i for formycin 5′-phosphate, a tight-binding competitive inhibitor. Isotope effects were measured as a function of the allosteric activator concentration that increases the turnover number of the enzyme from 0.006 s^{-1} to 1.2 s^{-1}. The kinetic isotope effects were measured with the substrates [1′-^{3}H]AMP, [2′-^{2}H]AMP, [2′-^{2}H]AMP, [9-^{15}N]AMP, and [1′,9-^{14}C, ^{15}N]AMP. All substrates gave significant kinetic isotope effects in a pattern that establishes that the reaction expresses intrinsic kinetic isotope effects in the presence or absence of MgATP. The kinetic isotope effect with [9-^{15}N]AMP decreased from 1.034 ± 0.002 to 1.021 ± 0.002 in response to MgATP. The [1′-^{3}H]AMP isotope effect increased from 1.086 ± 0.003 to 1.094 ± 0.002, while the kinetic isotope effect for [1′,9-^{14}C, ^{15}N]AMP decreased from 1.085 ± 0.003 to 1.070 ± 0.004 in response to allosteric activation with MgATP. Kinetic isotope effects with [1′-^{14}C]AMP and [2′-^{2}H]AMP were 1.041 ± 0.006 and 1.089 ± 0.002 and were not changed by addition of MgATP. Transition-state analysis using bond-energy and bond-order vibrational analysis indicated that the transition state for the mutant enzyme has a similar position in the reaction coordinate compared to that for the normal enzyme. The mutant enzyme is less effective in stabilizing the carbocation-like intermediate and in the ability to protonate N7 of adenine to create a better leaving group. This altered transition-state structure was confirmed by an altered substrate specificity for the mutant protein.

Treatment of *Azotobacter vinelandii* with nitrosoguanidine produced a cell strain that contains a V_{max} mutant of the AMP nucleosidase protein (Leung & Schramm, 1981). Other properties of the enzyme, including the K_m for AMP, activation by MgATP, and inhibition by formycin 5′-phosphate, were changed by less than 2-fold. Preliminary studies indicated that the mutant enzyme gave an altered family of heavy-atom kinetic isotope effects relative to the normal enzyme (Parkin & Schramm, 1984). Recently, we have established that the native AMP nucleosidase catalyzes a concerted reaction that expresses intrinsic kinetic isotope effects (DeWolf et al., 1986; Parkin & Schramm, 1987). The transition-state structures for acid- and enzyme-catalyzed hydrolysis of the N-glycosidic bond of AMP have been determined from the family of kinetic isotope effects (Mentch et al., 1987). For native AMP nucleosidase, transition-state analysis was used to establish that the transition state is altered by the action of the allosteric activator (Parkin & Schramm, 1987; Mentch et al., 1987). The results indicated that transition-state analysis can also be used to determine the nature of active-site mutations at the level of the transition-state structure.

In this study, isotope effects have been measured that establish that the V_{max} mutant of AMP nucleosidase expresses intrinsic kinetic isotope effects. Kinetic isotope effects were determined in the presence and absence of the allosteric activator. Transition-state structures were calculated by using the functions that relate the magnitude of kinetic isotope effects to the bond orders and vibrational force field of the transition state (Bigeleisen & Wolfsberg, 1958; Sims et al., 1977; Sims & Lewis, 1984). This experimental protocol can establish details of enzymatic transition-state structure for enzymes that express full kinetic isotope effects (Cleland, 1982; Scharschmidt et al., 1984). For mutant enzymes, or enzymes that have been altered by site-directed mutagenesis, this approach has the potential to provide information on the changes that occur in the transition state. Transition-state structures are not available from X-ray crystal structures or from NMR studies that report on the location and environment of specific atoms in stable reactant configurations. Studies with transition-state inhibitors also give structures that may approximate but differ from the actual transition state. Heavy-atom kinetic isotope effects offer the only method currently available to investigate enzymatic transition-state structure. Although several assumptions must be made about molecular motion in the transition state (Sims & Lewis, 1984), the correlation of theory with transition states for well-established chemical reactions provides confidence that such analyses have validity. Recent theoretical studies also provide evidence that these methods provide good approximations of transition-state structures (Huskey, 1991).

The results of this study establish that mutagenesis of AMP nucleosidase that decreases V_{max} also changes the nature of the transition state. Application of these methods to site-

† This work was supported by Research Grant GM 21083 from the National Institutes of Health. Postdoctoral fellowship support for B.A.H. was from Grant PF-3298 of the American Cancer Society and a Mildred and Emil Holland Scholarship. A portion of this work was performed in the Department of Biochemistry, Temple University School of Medicine, Philadelphia, PA 19140.
* To whom correspondence should be addressed.
‡ Current address: Department of Chemistry, Chestnut Hill College, Germantown Avenue, Philadelphia, PA 19118.
§ Current address, Wyeth-Ayerst Research, CN-8000, Princeton, NJ 08543.

0006-2960/91/0430-4586$02.50/0

Table I: Substrates for the Determination of Kinetic Isotope Effects with AMP Nucleosidase and a Summary of Isotope Effects in the Absence and Presence of MgATP[a]

substrates	isotope effect	abbr.	kinetic isotope effect[b] no ATP	kinetic isotope effect[b] 0.5 mM MgATP
[1′-^{14}C]AMP + [5′-^{3}H]AMP	primary ^{14}C	^{14}C1′	1.041 ± 0.006 (3)	1.041 ± 0.003 (3)
[9,5′-^{15}N, ^{14}C]AMP + [5′-^{3}H]AMP	primary ^{15}N	^{15}N9	1.034 ± 0.002 (9)	1.021 ± 0.002 (6)
[9,1′-^{15}N, ^{14}C]AMP + [5′-^{3}H]AMP	multiple primary ^{14}C–^{15}N	^{14}C1′ + ^{15}N9	1.085 ± 0.003 (3)	1.070 ± 0.004 (3)
[1′-^{3}H]AMP + [5′-^{14}C]AMP	α-secondary ^{3}H	^{3}H1′	1.086 ± 0.003 (3)	1.094 ± 0.002 (3)
[2′,5′-^{2}H, ^{3}H]AMP + [5′-^{14}C]AMP	β-secondary ^{2}H	^{2}H2′	1.089 ± 0.002 (6)	1.086 ± 0.002 (6)
[5′-^{3}H]AMP + [5′-^{14}C]AMP	control[c]	^{3}H5′		0.997 ± 0.002 (9)

[a] Isotope effects are classified as primary, the heavy atom is a bonding atom in the bond being broken; α-secondary, the heavy atom is in the α position relative to the bond being broken; and β-secondary, the heavy atom is in the β position relative to the bond being broken. [b] Data for the ^{14}C1′ and ^{3}H1′ isotope effects were reported previously (Parkin & Schramm, 1984) and are included for comparison. The number in parenthesis is the number of experimental determinations used for the average value and the standard deviation. [c] The ^{3}H5′ kinetic isotope effects for hydrolysis of AMP by acid and the native AMP nucleosidase were previously found to be 1.006 ± 0.002 (Parkin & Schramm, 1987; Mentch et al., 1987). The ^{3}H5′ isotope effect for the mutant enzyme differs in being close to unity. This finding was confirmed by determination of the ^{3}H5′ isotope effect in simultaneous experiments with the native and mutant enzymes. Since the ^{3}H5′ isotope effect is close to unity, no corrections were applied to the measured isotope effects. The control isotope effect with no ATP was not measured since other isotope effects in the ribose demonstrate minimal changes as a result of MgATP activation.

directed enzyme mutations should be valuable in understanding the role of individual amino acids in stabilizing specific transition-state structures.

Materials and Methods

Mutant AMP Nucleosidase. The strain of *Azotobacter vinelandii* that produces defective AMP nucleosidase was grown in 300-L batches in an airlift fermenter modified from that described previously (Schramm, 1974). Mixing and aeration were provided by air delivered through porous Teflon tubing. Purification of the mutant enzyme was based on published methods (Leung & Schramm, 1981) and the following modification. After the DEAE-Sephadex step, the enzyme was concentrated and further purified by Ultra-Gel 34 filtration chromatography with 0.1 M Tris-HCl, pH 8.0, containing 0.15 M KCl, 2 mM AMP, 0.1 mM dithiothreitol, and 0.1 mM EDTA as the eluant. The final step was on AMP-Sepharose as described previously (Leung & Schramm, 1981). The modification increased the specific activity of the purified enzyme to 0.6 μmol min^{-1} mg^{-1} protein compared to the previously reported specific activity of 0.3 μmol min^{-1} mg^{-1}, even though the previous preparation was nearly homogeneous by SDS–polyacrylamide gel electrophoresis. After storage for several years at −70 °C and numerous freeze–thaw cycles, the enzyme lost approximately 60% of its original activity. Kinetic isotope effects were independent of the specific activity of the enzyme preparation. Initial rate and kinetic isotope effect studies used homogeneous enzyme preparations with specific activities ranging from approximately 0.1 to 0.6.

Isotopically Labeled AMP. AMP substrates were labeled with radioactive and/or heavy atoms by the chemical and enzymatic methods described previously (Parkin & Schramm, 1987; Parkin et al., 1984). The isotopically labeled compounds used in this study are summarized in Table I.

Measurement of Kinetic Isotope Effects. Kinetic isotope effect experiments measured the relative rates of hydrolysis of AMP that contained heavy or natural-abundance isotopes at specific positions. In every case, one substrate contained ^{3}H and the other contained ^{14}C in the ribose portion of AMP. The ratio of ^{3}H/^{14}C in the product ribose 5-phosphate was used to calculate the kinetic isotope effects as previously detailed (Parkin & Schramm, 1987; Parkin et al., 1984). This competitive method gives information on V_{max}/K_m kinetic isotope effects, that is, the steps between free enzyme and substrate and the first kinetically irreversible step in the reaction. All kinetic isotope effects are expressed as the ratio of the natural abundance and heavy-atom kinetic isotope effects, i.e., (V_{max}/K_m for the light isotope)/(V_{max}/K_m for the heavy isotope). The nomenclature of atoms of AMP and the associated oxygen nucleophile in the enzyme-catalyzed transition state is shown in Figure 1. Abbreviations for specific heavy-atom kinetic isotope effects refer to the position of the label in AMP and the specific isotope substitution. The ^{3}H1′ kinetic isotope effect refers to the ratio of V_{max}/K_m for normal AMP and that with ^{3}H at the 1′ position. Kinetic isotope effects on ligand binding (if any) do not influence V_{max}/K_m isotope effects when the catalytic step is slow relative to substrate addition and release. Thus, intrinsic V_{max}/K_m kinetic isotope effects can be used to calculate the transition-state structure. These conditions have been established for native AMP nucleosidase (DeWolf et al., 1986; Parkin & Schramm, 1987) and are established here for the mutant enzyme.

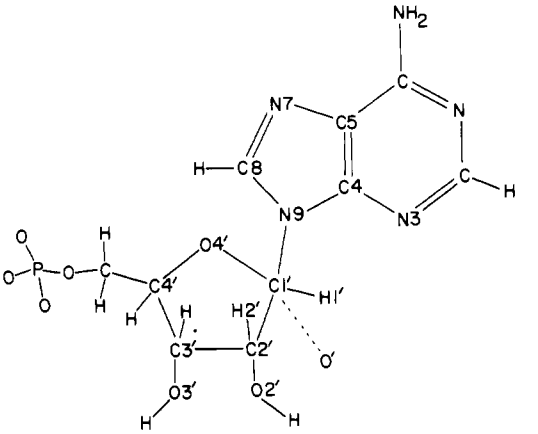

FIGURE 1: Structure of AMP and nomenclature of atoms surrounding the anomeric carbon of ribose 5-phosphate. The oxygen labeled O′ is the water (or hydroxyl) nucleophile that replaces adenine in this reaction. AMP is shown in the anti configuration around the glycosyl bond, its normal solution structure. The pK_a for N1 is 3.6, and the pK_a′ for N7 is <1 (Garrett & Mehta, 1972).

Substrate Activity of 8-BrAMP. The hydrolysis of 8-BrAMP to 8-Br-adenine and ribose 5-phosphate by mutant and native AMP nucleosidases was measured by high-performance liquid chromatography. Reaction mixtures of 50 μL (see Table III) were incubated at 30 °C for appropriate intervals with the native or mutant AMP nucleosidase. Samples were analyzed for 8-Br-adenine and 8-BrAMP. Control incubations contained the same components but without enzyme. The small amount (<0.5%) of 8-Br-adenine formed nonenzymatically in overnight incubations of the control was subtracted from the enzymatic rates.

Calculations of Transition-State Structures. The BEBOVIB-IV program [Quantum Chemistry Program Exchange No.

Table II: Comparison of Single and Multiple Kinetic Isotope Effects for the Mutant AMP Nucleosidase

	individual isotope effects		combined $^{14}C1'$ and $^{15}N9$ isotope effect		
			predicted isotope effect		
reaction condition	$^{14}C1'$	$^{15}N9$	stepwise[a]	concerted[b]	obsd
no ATP	1.041 ± 0.006	1.034 ± 0.002	1.040 ± 0.006	1.076 ± 0.007	1.085 ± 0.003
0.5 mM MgATP	1.041 ± 0.003	1.021 ± 0.002	1.041 ± 0.004	1.063 ± 0.004	1.070 ± 0.004

[a] For a reaction in which two bond breaking steps (transition states) contribute to the observed isotope effect. The predicted isotope effect for a stepwise mechanism is given by $(^{14}C1' - 1)/(^{14}C1'$ and $^{15}N9$ combined $- 1) = {}^{15}N9/{}^{15}K_{eq}$ (Cleland, 1987). For AMP hydrolysis, $^{15}K_{eq}$ is calculated to be 1.012 based on the reported distribution of N7 and N9 tautomers (Dreyfus et al., 1975) and BEBOVIB calculations using the calculated bond orders for each tautomer (Wiórkiewicz-Kuczera & Karplus, 1990). This expression is for $^{15}N9$ and $^{14}C1'$ effects that occur in different steps. Distinct steps for AMP nucleosidase would be unlikely since $^{14}C1'$ and $^{15}N9$ isotope effects are required to occur together in the initial C–N bond cleavage. [b] For a concerted mechanism in which all isotope effects arise from a single transition state, the predicted isotope effect is given by ($^{14}C1'$ isotope effect) × ($^{15}N9$ isotope effect) (Hermes et al., 1982).

337, Sims et al. (1977)] was used to determine the transition-state structures that correspond to the measured kinetic isotope effects. Isotopic substitutions at C1′, N9, H1′, and H2′ were examined. Kinetic isotope effects were calculated, relative to a fixed reactant-state structure of AMP, for families of transition states that differ in one or more structural details. Comparison of measured and calculated kinetic isotope effects determines the transition-state structures that are consistent with the experimental results.

Bond lengths and angles for the reactant AMP molecule were taken from X-ray data (Kraut & Jensen, 1963). Force constants for bond stretching, valence angle bending, and torsional rotation are estimated from tabulated values (Sims & Lewis, 1984; Wilson et al., 1955). The AMP atomic reactant model includes all atoms within two bonds of the cleaving C1′–N9 bond of AMP, the atoms constituting the imidazole portion of adenine, and the ribosyl portion of the nucleotide, with the exception of atoms O3′ and H3′. The hydroxylic hydrogens are excluded in the model, since trial calculations indicated that they made no significant contribution to the calculated kinetic isotope effects. The AMP transition-state models include all atoms used in the reactant model, the attacking oxygen nucleophile, and, when appropriate, a H that protonates N7. Replacement of a vibrational motion of the reactant model with a translational separation of the adenine and ribose produces a reaction coordinate for the transition-state model. Families of transition states were characterized that vary in the degree of bond breaking to N9, the extent of participation of a water nucleophile (O′ in Figure 1), the relative degree of carbonium ion stabilization by conjugation and hyperconjugation, the extent of protonation at N7, the various conformations of the ribose ring, and the angle of the attacking oxygen nucleophile. The bond-angle and bond-length changes associated with these structural modifications are translated into changes in stretching and bending force constants by using the approach of Sims & Lewis (1984). A more detailed description of the application of these rules to AMP hydrolysis is found in recently published work (Mentch et al., 1987). The effects of various assumptions on the calculated isotope effects are discussed by Huskey (1991). The results reported here extend the reactant and transition-state models by including a closed ribosyl ring and including the ribose configuration at C2′ and C4′. The ribose conformation in the transition state is modeled similarly to that for the crystal structure of ribonolactone, which has sp^2 hydridization at C1′ (Kinoshita et al., 1981). The transition-state models included a shortened C1′–H1′ bond and an out-of-plane bending mode for H1′ to reflect the sp^2 hydridization at C1′. The effect of the angle of attack of the water nucleophile (O′ in Figure 1) on the isotope effect was also considered. The direction of the water attack had a small influence on the calculated kinetic isotope effect until the oxygen was more than 20 ° out-of-line from the direction of the breaking C1′–N9′ bond. Thus, all models were made with the assumption that the attacking O′ was 180° from the departing adenine.

The BEBOVIB-IV program has been modified to run on IBM-compatible and MacIntosh personal computers, the Silicon Graphics Personal Iris workstation, and the 4D/80S and 4D/240 Silicon Graphics processors. Typical computational times to obtain the kinetic isotope effects for 16-atom transition states are 40 min, 5 min, 2 min, 15 s, and 5 s for the ATT 6300 1 MB with math coprocessor, MacIntosh II with 5 MB and math coprocessor, MacIntosh II ci, and Silicon Graphics 4D/80S and 4D/240 processors, respectively.

Results

Kinetic Isotope Effects. The AMP substrates used for kinetic isotope effect determinations are summarized in Table I. Kinetic isotope effects were measured in the absence of MgATP and at increasing activator concentrations to 0.5 mM. The activation constant for MgATP is near 22 μM, and the response of initial reaction rates to the activator concentration is strongly sigmoidal. A concentration of 0.5 mM MgATP is near saturation. Values for the V_{max}/K_m kinetic isotope effects are given in Table I. The response of kinetic isotope effects to allosteric activation is illustrated in Figure 2. All substrates labeled with heavy atoms gave kinetic isotope effects that were normal (AMP containing the heavy isotope reacts more slowly) and significant compared to the standard errors of the measurement or to control experiments with both ^3H and ^{14}C in the isotopically "insensitive" positions (the 5′ position of AMP). The control kinetic isotope effect of 0.997 ± 0.002 with $^3H5'$ differs from the value of 1.006 ± 0.002 established for this reaction when catalyzed by acid or the native enzyme (Parkin & Schramm, 1987). Separate experiments established the significance of this difference (footnote *b*, Table I).

Activation by MgATP had no effect on the $^2H2'$ and $^{14}C1'$ kinetic isotope effects but caused a slight increase in the $^3H1'$ effect and a substantial decrease from 1.034 to 1.021 in the $^{15}N9$ kinetic isotope effect. The decrease in the $^{15}N9$ kinetic isotope effect was verified in the combined $^{14}C1' + {}^{15}N9$ kinetic isotope effect, which decreased from 1.085 to 1.070 as a function of MgATP (Table I). Since the isotope effect at $^{14}C1'$ is not influenced by MgATP activation, the decrease must be attributed to the $^{15}N9$ effect. The change in the $^{15}N9$ kinetic isotope effect is abrupt and corresponds to the MgATP concentration that causes the allosteric transition (Figure 2).

The multiple kinetic isotope effect experiments with $^{14}C1'$ and $^{15}N9$ labels in the same substrate are compared to the products of the individual kinetic isotope effects in Table II. The combined kinetic isotope effects are slightly larger than those predicted from the individual isotope effects. However, the differences are not highly significant when considering the

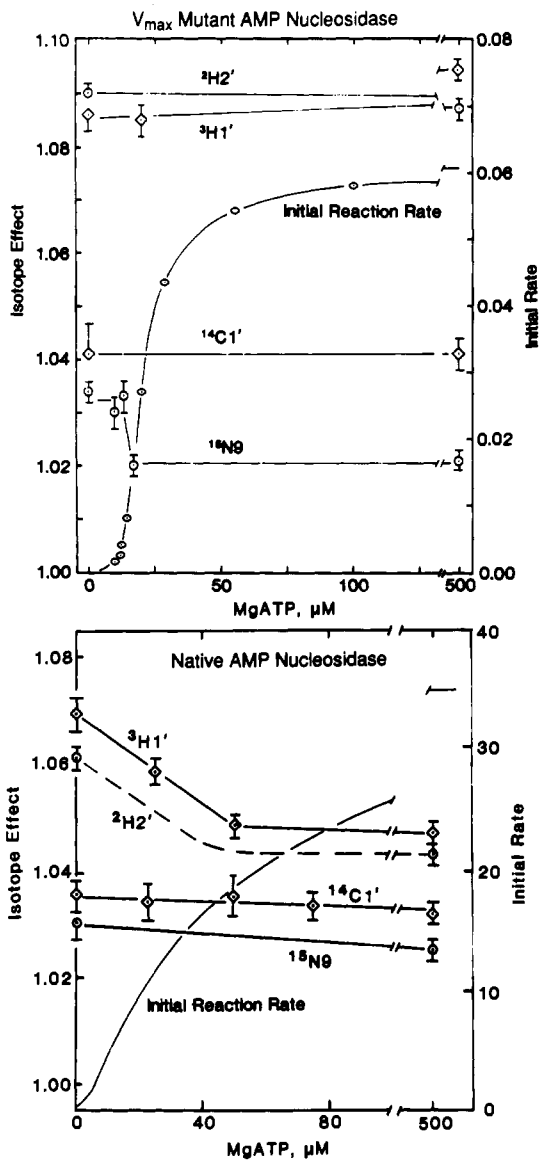

FIGURE 2: Kinetic isotope effects for the mutant and native AMP nucleosidases as a function of MgATP, the allosteric activator. The upper panel presents data for the mutant enzyme. The line labeled "Initial Reaction Rate" indicates the change in the initial rates of product formation as a function of MgATP. In the absence of MgATP the rate is 0.005 times that of the maximum rate when AMP is maintained at 0.5 mM. The concentration of AMP was near 1 mM in experiments to determine the kinetic isotope effects. Data for the $^3H1'$ and $^{14}C1'$ isotope effects at 0 and 500 μM MgATP were reported previously (Parkin & Schramm, 1984) and have been corrected for the actual $^3H5'$ isotope effect with the mutant enzyme. The error bars are two standard deviations of the mean. The lines were drawn by eye to fit the experimental points. The number of determinations for each isotope effect is given in Table I. The isotope effect (left ordinate scale) is the experimentally measured isotope effect adjusted for the fraction of the substrate converted to products. The initial rate results are from Leung and Schramm (1981). The lower panel shows data for the native enzyme and includes the isotope effects reported by Parkin and Schramm (1984, 1987) for comparison with the mutant enzyme.

experimental errors of the product of the individual kinetic isotope effects. Combined kinetic isotope effects smaller than the product of the individual effects would be indicative of multiple steps with similar energy barriers. The results of Table II establish that the primary heavy-atom kinetic isotope effects arise from the same step in catalysis.

The kinetic isotope effects for native AMP nucleosidase are given in the lower panel of Figure 2 for comparison with those obtained with the mutant enzyme. The magnitude of the

Table III: Comparison of 8-BrAMP as a Substrate for the Mutant and Native AMP Nucleosidase[a]

		k_{cat} (mol s^{-1} mol^{-1} enzyme)[b]		
enzyme	condition	AMP	8-BrAMP	k_{cat} (AMP)/ k_{cat} (8-BrAMP)
native	no ATP	0.3	$<2 \times 10^{-5}$	$>1.5 \times 10^4$
	+ MgATP	62.0	$<2 \times 10^{-5}$	$>3.1 \times 10^6$
mutant	no ATP	0.006	$<2 \times 10^{-5}$	$>3 \times 10^2$
	+ MgATP	1.2	0.009	1.3×10^2
control	+ MgATP, FMP[c]	$<2 \times 10^{-5}$	2×10^{-4}	

[a] Reaction mixtures contained 1 mM 8-BrAMP, 0.1 M triethanolamine, pH 8.0, 30 mM KCl, 10 mM $MgCl_2$, and where indicated 0.5 mM ATP and 1.0 mM formycin 5'-phosphate (FMP). The enzyme concentration was 0.29 mg/mL for both reactions. Samples were analyzed by HPLC after 1, 2, 3, 5, and 23 h at 30 °C. [b] The functional catalytic unit of the native AMP nucleosidase is a dimer of molecular weight 110 000, and the assumption is made that the mutant enzyme is similar, based on molecular weight studies (Leung & Schramm, 1981). The k_{cat} values for the native and mutant enzymes have been corrected for the control rate of 8-BrAMP hydrolysis, determined to be 2×10^{-4} based on the control experiment at 23 h. The control rate is expressed in the same units for easy comparison even though no enzyme was present in the control samples. [c] Formycin 5'-phosphate is a competitive inhibitor with $K_i \cong 40$ nM for both enzymes. The control rate of 8-BrAMP hydrolysis was determined in the presence of the mutant enzyme, inhibited by FMP.

kinetic isotope effects and their responses to allosteric activation by MgATP differ substantially for native and mutant enzymes.

Altered Substrate Specificity for the Mutant AMP Nucleosidase. The AMP analogue 8-BrAMP was compared as a substrate for native and mutant AMP nucleosidases. The results (Table III) indicate that the native enzyme hydrolyzes 8-BrAMP with a turnover number of less than 2×10^{-5} s^{-1} in the presence or absence of the allosteric activator. The rate is less than 0.0003% of the hydrolytic rate with AMP. The mutant enzyme hydrolyzes 8-BrAMP with a turnover number of 9×10^{-3} s^{-1} in the presence of MgATP, 0.7% as well as it hydrolyzes AMP. Control experiments that contained formycin 5'-phosphate, a strong competitive inhibitor of both the native and mutant AMP nucleosidases, inhibited 98% of the catalytic activity of the mutant enzyme activity with 8-BrAMP. Conversion of 8-BrAMP to 8-Br-adenine is thus an inherent activity of mutant AMP nucleosidase. The mutant enzyme required MgATP for the conversion, also indicative of AMP nucleosidase action. Extended incubations of the mutant and native enzymes with 1 mM 8-BrAMP gave a 16% enzymatic conversion of the substrate to 8-Br-adenine for the mutant enzyme, while no detectable enzymatic product (<0.2%) was formed with native enzyme.

Transition-State Structures for the Mutant AMP Nucleosides. The kinetic isotope effects summarized in Table I correspond to the transition-state structures given in Figure 3. The agreement between calculated kinetic isotope effects for specific transition states obtained with the BEBOVIB-IV program and the experimentally determined values is shown in Table IV. In the absence of ATP, two transition-state structures were found that correspond to the experimental isotope effects. One transition-state structure for the reaction without ATP lacks protonation of N7 in the transition state and has a C1'–N9 bond order of 0.094 and a O'-C1' bond order of 0.026. The other transition state in the absence of ATP is protonated at N7 and has a C1'–N9 bond order of 0.04 and a O'–C1' bond order of 0.06 (see Figure 3). In the presence of MgATP, only one transition-state structure was

Table IV: Comparison of Experimental Kinetic Isotope Effects for the Mutant AMP Nucleosidase with the Calculated Effects for Specific Transition-State Structures[a]

	no ATP			with ATP	
		calcd			
isotope effect calcd[d]	expl	C1′–N9 = 0.094[b]	C1′–N9 = 0.04[c]	expl	calcd
^{14}C1′	1.041 ± 0.006	1.041	1.040	1.041 ± 0.003	1.039
^{3}H1′	1.086 ± 0.003	1.087	1.087	1.094 ± 0.002	1.096
^{15}N9	1.034 ± 0.002	1.034	1.034	1.021 ± 0.002	1.023
^{2}H2′	1.090 ± 0.002	1.090	1.091	1.086 ± 0.002	1.085

[a] Bond orders were systematically varied in the transition-state structures and the expected kinetic isotope effects calculated with the BEBOVIB-IV program as described under Materials and Methods. [b] The calculated kinetic isotope effects correspond to the unprotonated structure at N7, which is labeled "Transition State, No ATP" in Figure 3. [c] The calculated kinetic isotope effects correspond to the protonated structure at N7, which is labeled "Transition State, No ATP" in Figure 3. [d] Only one chemically reasonable transition-state structure was found to correspond to the experimental results obtained in the presence of MgATP and is labeled "Transition State, with ATP" in Figure 3.

found that satisified the measured isotope effects. Protonation of N7 by an enzymatic group and a bond order of 0.18 for the C1′–N9 bond and 0.006 for the O′–C1′ bond are the major characteristics of this transition state.

Discussion

Evidence for Intrinsic Heavy-Atom Kinetic Isotope Effects. Kinetic isotope effects with the V_{max} mutant of AMP nucleosidase from *A. vinelandii* are characteristic of reactions with concerted bond cleavage that give intrinsic kinetic isotope effects. These include (a) constant kinetic isotope effects for ^{2}H2′ and ^{14}C1′ as the turnover number of the enzyme is altered by 240-fold, (b) a change in the opposite directions for the ^{3}H1′ and ^{15}N9 kinetic isotope effects as the reaction rate is altered by allosteric activation, (c) expression of the ^{15}N9 and ^{2}H2′ isotope effects near the theoretical limit for the isotope mass with chemically reasonable transition states, and (d) multiple kinetic isotope effects being the product of the individual isotope effects. These features do not prove the presence of full intrinsic isotope effects. However, any kinetic commitment that decreases the observed isotope effects must be coincidentally compensated by changes in transition-state structure to decrease only the ^{15}N9 effect while increasing the ^{3}H1′ effect with no change in the ^{2}H2′ and ^{14}C1′ effects. Thus, we can conclude that intrinsic or very nearly intrinsic isotope effects are observed. When intrinsic isotope effects are observed, the transition-state structure can be established by a systematic search of bond orders, bond angles, and vibrational frequencies for the transition state that corresponds to the family of measured kinetic isotope effects (Sims & Lewis, 1984). This theory has been applied to a number of chemical reactions and more recently to several enzymatic reactions (Mentch et al., 1987; Sims & Lewis, 1984; Rodgers et al., 1982; Markham et al., 1987). Comparison of enzymatic transition states where the catalyst has been changed by allosteric modifiers (Mentch et al., 1987), essential cofactors (Markham et al., 1987) or, as reported here, by mutation of the protein provides new insight into the nature of catalysis and its regulation.

The ^{3}H/^{14}C competitive method of measuring isotope effects measures V_{max}/K_m and therefore gives information on the collection of intermediates between the free enzyme and substrate and the first irreversible step in the catalytic mechanism (Northrop, 1981). For the native AMP nucleosidase, the first irreversible step is the conversion of AMP to products on the enzyme, since this equilibrium strongly favors products (DeWolf et al., 1986). The equilibrium of enzyme-bound intermediates has not been directly determined for the mutant enzyme. However, the isotope effects clearly establish bond breaking as the highest energy barrier in the V_{max}/K_m profile since both the ^{15}N9 and ^{2}H2′ isotope effects are near the maximum theoretical values for reasonable S_N1 transition states for N-glycosidic bond hydrolysis. Reaction reversal is not a factor since product release is irreversible during initial rate measurements (DeWolf et al., 1986). Isotope effects on the binding of substrates [if any, see LaReau et al. (1989)] do not alter the meaning of V_{max}/K_m isotope effects, since V_{max}/K_m effects report on the enzyme-equilibrium vibrational-energy differences between the free substrate and the bound transition state. Thus, the observed isotope effects for the mutant AMP nucleosidase are likely to be intrinsic effects associated with chemical cleavage of the N-glycosidic bond in a single step.

Table V: Expected Isotope Effects for AMP Glycoside Bond Hydrolysis with S_N1 or S_N2 Transition-State Structures[a]

	transition-state structure	
isotope effect	S_N1	S_N2
^{14}C1′	1.04	1.10
^{15}N9	1.03	1.02
^{3}H1′	1.28	1.02
^{2}H2′	1.08	1.00

[a] The S_N1 transition state that gives these isotope effects has a C1′–N9 bond order of 0.05, with concommitant development of carbocation character in C1′–O4′. There is no participation of C1′–O′ bonding, and the N7 of adenine is protonated in the transition state. The S_N2 transition state that gives these isotope effects has C1′–N9 and C1′–O′ bond orders of 0.5. The data are taken from BEBOVIB-IV calculations. The methods are summarized in Mentch et al. (1987), and these data are taken from calculations used for Figure 2 of Mentch et al. (1987).

Qualitative Features of the Transition States. Transition states for *N*-glycoside hydrolysis with S_N1 and S_N2 characteristics give families of kinetic isotope effects in the ranges shown in Table V, which can be compared to those for the mutant AMP nucleosidase in Table I. The enzymatic reaction differs from both, although features of both can be found. The ^{2}H2′ isotope effect of greater than 1.08 clearly eliminates a transition state with strong nucleophilic character or any mechanism with compression of bonds in the reaction coordinate around C1′ in the transition state. Weak reaction coordinate bonds to C1′ indicate a strong carbocation character in the ribose ring. Acid-catalyzed solvolysis of glucosyl pyranosides, which is known to give S_N1-like transition states, gives ^{2}H2′ β-secondary isotope effects of 1.080 (Bennet & Sinnott, 1986). The ^{3}H1′ effect of 1.09 is smaller than that predicted for classic S_N1 transition states but larger than that of S_N2-like transition states, indicating that the out-of-plane motion of H1′ is restricted in the enzymatic transition state. By comparison, the acid-catalyzed solvolysis of AMP gives a ^{3}H′ effect of 1.23 (Parkin & Schramm, 1984; Parkin et al., 1984). The decreased ^{3}H1′ isotope effect clearly invokes the participation of a water nucleophile as shown in Figure 3. Isotope effects with ^{14}C1′ are near 1.04 and indicate modest reaction coordinate motion of C1′ in the transition state, resembling the S_N1-like transition state. Symmetric S_N2 tran-

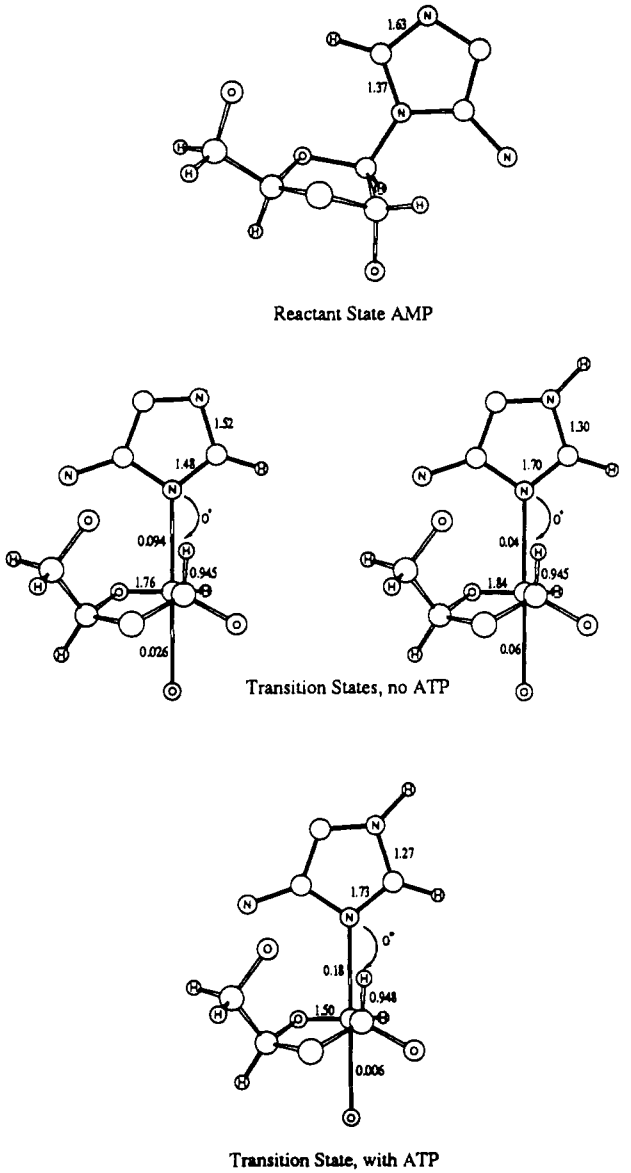

FIGURE 3: Proposed transition-state structures for the mutant AMP nucleosidase. The structure "Reactant State AMP" is taken from the crystal structure of AMP (Krant & Jensen, 1963) and is unprotonated at N7 at pH 8.0 ($pK_a \sim 1$). The conformation around the glycosidic bond is anti. All atoms two bonds or more from the C1′–N9 bond are shown and were used in the calculations for kinetic isotope effects. The bond orders for N9–C8 and C8–N7 are 1.37 and 1.63, respectively, in the reactant state. The glycosidic bond order and bond orders in ribose are taken to be 1.00 in the reactant AMP. The unmarked atoms are carbons. The structures labeled "Transition States, no ATP" are the two transition-state structures that correspond to the kinetic isotope effects in the absence of the allosteric activator. The total bond order to C1′ is 3.9 for the structure on the left and 3.8 for the structure on the right for "Transition States, no ATP". The attacking water oxygen nucleophile is attacking from below the ribose ring, 180° from the departing adenine in a linear reaction coordinate. The structure on the left has not been protonated at N7 by the enzyme, while the structure on the right is protonated. The conformations around the glycosidic bonds are syn for the transition states with no ATP. The structure "Transition State, with ATP" is the structure that corresponds to the kinetic isotope effects in the presence of 0.5 mM MgATP. The total bond order to C1′ is 4.0 for "Transition State, with ATP". A major difference between the middle-left and lower structure is the protonation of N7 by an acidic group of the enzyme, causing redistribution of bond order in the imidazole ring. The bond order to the departing adenine is higher in the presence of ATP, indicating an earlier transition state. The increased bond order in N9–C1′ is accompanied by decreased bond order in the C1′–O4′ bond. The bond lengths are drawn to scale by using Pauling's rule (bond length = single bond length − 0.3 ln x, where x is the bond order).

sition states can give ^{14}C1′ isotope effects greater than 1.10, with reported effects as large a 1.16 but more commonly near 1.10 (Mentch et al., 1987; Rodgers et al., 1982; Melander & Saunders, 1980; Markham et al., 1987). The ^{15}N9 effect is 1.034 and decreases to 1.021 in the presence of the allosteric activator. The value of 1.034 is the maximum expected ^{15}N effect for an S_N1 mechanism and is near the theoretical limit of 1.04 for a change of 1.0 in the total bond order to N9 (Mentch et al., 1987). This value reports on the total bonding to N9 in the transition state, with loosely bound N giving rise to the largest kinetic isotope effects. Since both the extent of C1′–N9 bond breaking and the protonation of the adenine ring influence the bonding to N9 in the transition state, the ^{15}N isotope effect does not discriminate well between associative and dissociative mechanisms. However, the large isotope effect establishes that bonding to N9 in the transition state is weak relative to that in the ground state and that the bonding increases under conditions of allosteric activation.

Combined Heavy-Atom Isotope Effects. The combined isotope effect with ^{14}C1′ and ^{15}N9 labels in the same molecule was slightly larger than the product of the individual isotope effects both in the presence and absence of allosteric activation. The activator-induced decrease in the ^{15}N9 isotope effect was also observed in the combined isotope effect. If C–N bond breaking occurs in a stepwise fashion with one transition-state barrier for C–N breaking and a second barrier of similar energy for a second transition state that involves only the ^{14}C isotope effect, the ^{14}C effect would partially obscure the combined ^{14}C–^{15}N9 effect, reducing the observed effect to less than the product of the individual isotope effects (Mentch et al., 1987; Cleland, 1987). This would occur if, for example, the enzyme formed a covalent ribosyl intermediate as is proposed for β-galactosidase and other *O*-glycohydrolases (Sinnott, 1987; Elliott et al., 1988) as well as NAD glycohydrolase (Schuber et al., 1976). The results (Table II) demonstrate that the carbon and nitrogen isotope effects arise from a single step, since the large effects for a carboxonium-like transition state would be unlikely to be generated in two sequential steps. Kinetic and chemical evidence has also demonstrated that the native AMP nucleosidase catalyzes a concerted reaction mechanism (DeWolf et al., 1986). On the basis of this precedent and the combined isotope effects, a concerted mechanism for the mutant enzyme is likely.

Quantitative Transition States for the Mutant AMP Nucleosidase. The transition-state structures that conform to the kinetic isotope effects and other features of catalysis by the mutant AMP nucleosidase are compared to the reactant-state AMP, based on the X-ray crystal structure (Figure 3). The conformation of AMP in solution is anti with respect to rotation around the C1′–N9 bond, with the C1′–O4′ and N9–C8 bonds approximately cis in this configuration. The relatively tight binding of formycin 5′-phosphate to both the normal and mutant enzymes ($K_m/K_i = >10^3$) indicates that the enzymes prefer to bind nucleotides in the syn configuration, similar to the crystal structure of formycin 5′-phosphate (Giranda et al., 1988). In this configuration, the C1′–O4′ and N9–C8 bonds are approximately trans, as indicated in the middle and lower structures of Figure 3. The syn configuration of formycin 5′-phosphate in the crystal is stabilized by a hydrogen bond between a phosphoryl hydroxyl and the nitrogen corresponding to N3 of AMP. A similar bonding could occur with enzyme-bound AMP.

Kinetic isotope effects for ^{14}C1′ and ^{2}H2′ are independent of activation by MgATP, indicating that net bonding of these atoms in the transition state is not influenced by allosteric

activation. The altered ^{15}N9 and ^{3}H1′ isotope effects indicate that allosteric changes increase the bonding to N9 in the adenine ring and cause a slightly greater freedom of motion for ^{3}H1′ in the transition state. In the absence of the activator, one proposed transition-state structure (left structure of Figure 3) includes a weak bond order of 0.094 from C1′ to N9. Increasing the C1′–N9 bond order or increasing the N9–C8 bond order beyond 1.48 decreased the calculated ^{15}N9 isotope effect significantly below the experimental value of 1.034 ± 0.002. This transition state indicates that the mutant enzyme has lost the ability to protonate N7 in the transition state in the absence of allosteric modification.

Another transition-state structure that corresponds to the isotope effects in the absence of ATP has bond orders reversed in the reaction coordinate and includes protonation of N7. These bond orders correspond to O′–C1′ = 0.06, C1′–N9 = 0.04, N9–C8 = 1.70, and O′4–C1′ = 1.84. The bond orders of this transition state are less reasonable than those for the transition state with unprotonated adenine as a leaving group. The oxycarbonium intermediate for acid-catalyzed solvolysis has an O4′–C1′ bond order of 1.71 (Mentch et al., 1987). The O4′–C1′ bond order of 1.84 is unreasonably large to represent the transition state for AMP nucleosidase.

How can the mutant AMP nucleosidase catalyze even the observed rate of 0.006 s^{-1} for adenine departure without the assistance of N7 protonation? The crystal structure of formycin 5′-phosphate demonstrates that the 5′-phosphate forms an internal hydrogen bond between the phosphate hydroxyl and N3 of the purine-analogue ring (Giranda et al., 1988). If AMP is bound to the enzyme in the syn configuration, similar to the crystal structure of formycin 5′-phosphate, internal N3 hydrogen bonding would be promoted and would facilitate adenine departure without protonation of N7. In the acid-catalyzed solvolysis of adenosine, rate constants have been proposed for both monoprotonated and diprotonated adenine, demonstrating that monoprotonation is sufficient for adenine departure (Garrett & Mehta, 1972) even though the rates are slow. These results suggest that the enzyme enforces formation of an internal hydrogen bond between N3 and the 5′-phosphate to promote catalysis. This bonding pattern can explain the absolute requirement for the 5′-phosphate for catalysis (DeWolf et al., 1979). Since N1 is the most basic nitrogen of the adenine ring, it is also possible that the mutant enzyme may protonate N1 and hydrogen bond to N3 to assist in adenine departure. Enzyme-enforced intramolecular bonding has also been proposed for the reactions catalyzed by dehydroquinate synthase (Bender et al., 1989) and aspartate carbamoyl transferase (Gouaux et al., 1987).

Effect of Allosteric Activation. Allosteric activation by MgATP changes both the ^{15}N9 and the ^{3}H1′ kinetic isotope effects to a significant extent. This pattern occurs as a consequence of changes in bonding in both the adenine ring and the reaction coordinate bonding. Protonation of N7 increases the N9–C8 bond order by approximately 0.3 based on X-ray crystal structures of N7–protonated and unprotonated purines (Zoltewicz et al., 1970; Taylor & Kennard, 1982). The excess bond order in C1′–O4′ decreases from 1.76 to 1.50, reflecting an earlier transition state that requires less development of the oxycarbonium intermediate.

Isotopic substitution in the ribose ring gave kinetic isotope effects that were independent of the presence of MgATP except for a small increase from 1.086 to 1.094 in the ^{3}H1′ effect. The change in the ^{3}H1′ effect represents an increase in bond order to the departing adenine and a decrease to the incipient water nucleophile. These changes provide an earlier transition

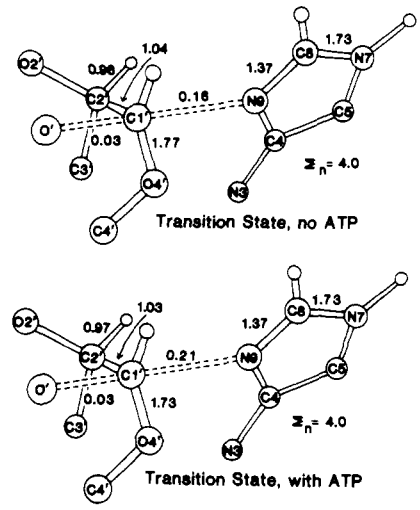

FIGURE 4: Transition states for the native AMP nucleosidase. The reactant state (not shown) for AMP is the same as in Figure 3. The transition states of the native enzyme are taken from Mentch et al. (1987), where complete descriptions are given together with the isotope effects used to establish these transition states.

state than in the absence of the allosteric activator. This result is similar to the native enzyme, where allosteric activation also causes the stabilization of an earlier transition state (Mentch et al., 1987). The transition-state structures for the native AMP nucleosidase are given in Figure 4 for comparison with those for the mutant enzyme in Figure 3.

Low bond orders to the leaving adenine group and the incipient oxygen nucleophile are required to accommodate the hyperconjugation that develops in the ribose ring as indicated by the large ^{2}H2′ isotope effect. Parameters that influence the ^{14}C1′ isotope effect are the total bond order to C1′ and the symmetry of the bonds in the reaction coordinate (O′–C1′–N9). Symmetric bonds of higher order increase the isotope effect, while asymmetry and decreased bond order decrease the isotope effect (Mentch et al., 1987). The calculated ^{3}H1′ effects vary from 1.40 to near 1.00 as the contributions of the O′–C1′ and C1′–N9 bonds each increase from 0 to 0.5 bond order in the transition state. The large ^{2}H2′ effect establishes that the ribose ring is oxycarbonium-like at the transition state. The ^{3}H1′ isotope effect establishes the restriction on the out-of-plane bending mode of H1′ in the transition state, which is the major source of the ^{3}H1′ isotope effect. With all isotope effects considered, only the transition-state structures shown in Figure 3 or others that are closely related could account for the experimental kinetic isotope effects for the mutant AMP nucleosidase. The simplest explanation for the changes in the presence of MgATP is a more favorable positioning of the acidic group on the enzyme that protonates N7.

Substrate Specificity. Acid-catalyzed solvolysis of 8-substituted adenosines demonstrates that the reactivity of 8-Br-adenosine > adenosine > 8-methoxyadenosine. These results have been interpreted as an inductive effect that aids the addition of the second proton at N7, resulting in the reactive dication (Garrett & Mehta, 1972). The mutant AMP nucleosidase appears to be defective in the ability to protonate the adenine leaving group. Thus, 8-BrAMP should be a better substrate for the mutant enzyme if the catalytic defect is protonation of the leaving group.

The mutant enzyme hydrolyzes 8-BrAMP at 0.54 min^{-1}, while the reaction rate was less than 0.0012 min^{-1} for the native enzyme, well below the limits of detection. This change in specificity is more pronounced when compared against the

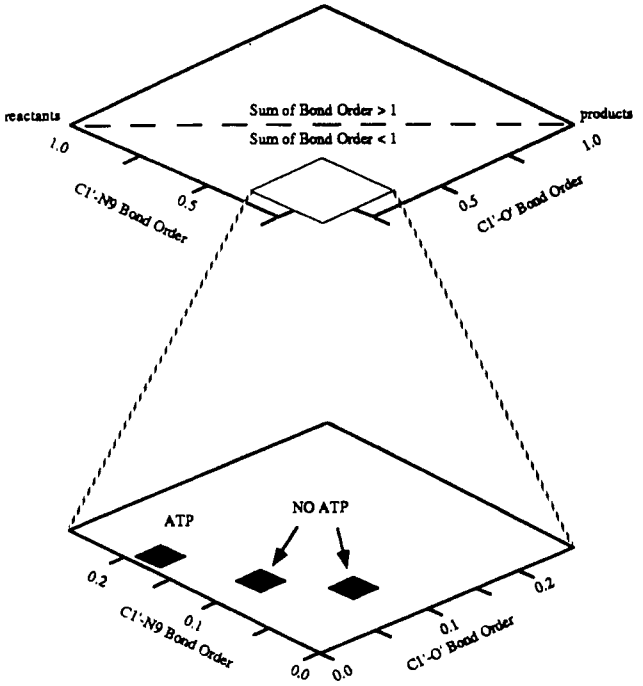

FIGURE 5: Transition-state diagram showing calculated transition-state structures for AMP hydrolysis by the mutant AMP nucleosidase. Any line connecting the reactant corner of the upper figure with the product corner represents a possible reaction pathway for AMP hydrolysis. A point in the two-dimensional coordinate space represents a transition-state structure with coordinates defined by the C1′–N9 and C1′–O′ bond orders. The dotted line in the upper figure defines a pathway in which the sum of the C1′–N9 and C1′–O′ bond orders is 1.0, a concerted S_N2 mechanism. Each point below the dotted line describes a structure in which bond forming lags behind bond breaking. The S_N1 formation of a carbocation is defined by the point (0.0, and 0.0). The lower figure, an enlargement of a portion of the upper plane, shows the coordinates of the transition-state structures that yield calculated kinetic isotope effects consistent with the experimental values. The figure illustrates the considerable carbocation character found in each transition-state structure as well as the inverted bond order relationship of the two families of structures for the hydrolysis of AMP in the absence of the allosteric activator MgATP.

rates of AMP hydrolysis for the mutant and native enzymes. When normalized for AMP hydrolysis, the mutant enzyme hydrolyzes 8-BrAMP greater than 2.4×10^4 times as rapidly as the native enzyme. These measurements confirm that the altered transition state measured with kinetic isotope effects is also expressed in the enzymatic substrate specificity.

Reaction Coordinate Space. The possible transition-state structures for the mutant AMP nucleosidase are well-defined in reaction coordinate space (Figure 5). The possible transition-state structures are confined to a small region that is S_N1-like and has low but significant preassociation of the water nucleophile. Not shown in Figure 5 are the changes in bonding at N9 or the changes in bond order in the ribose or adenine rings. One effect of the allosteric change on the transition state is to confer competence on the protonating group. Experimental identification of the protonating group(s) by the pH dependence of kinetic constants in the presence and absence of MgATP is limited by enzyme availability since the turnover number is approximately 0.01 s^{-1} at pH 8.0 in the absence of MgATP.

Much of the catalytic potential of AMP nucleosidase comes from the ability to stabilize the developing charge on O4′ of the ribose group. Stabilization of a positive charge on O4′ by ion pairing with a putative enzymatic anion alters the hyperconjugation to H2′ and the observed bond order at C1′–C2′ in the native enzyme (Mentch et al., 1987). In the mutant enzyme, the ^{2}H2′ kinetic isotope effect is more than double that for the native enzyme, indicating that O4′ ion pairing is less effective. The ^{2}H2′ isotope effect for the mutant enzyme is near that observed for nonenzymatic hydrolysis of AMP (Mentch et al., 1987). Thus, a second defect in the mutant enzyme is a decreased ability to stabilize the oxycarbonium intermediate.

Comparison of the Mutant and Native Transition States. The transiton-state structures for the native and mutant AMP nucleosidases are at approximately the same position in the reaction coordinate. The major difference in catalytic efficiency can be attributed to an altered ability to protonate N7 in the absence of the allosteric activator and differences in the ability to stabilize the developing positive charge in the ribosyl group. Addition of the allosteric activator to the native enzyme causes hyperconjugative redistribution in the ribose ring that is expressed primarily as a decrease in the ^{2}H2′ isotope effect. The larger ^{2}H2′ isotope effect for the mutant enzyme, which is unchanged by MgATP, establishes a decreased ability of the enzyme to stabilize the oxycarbonium intermediate. Thus, the O4′–C1′ bonds in the transition states for the native enzyme have bond orders of 1.77–1.73 while in the mutant enzyme these bonds are 1.76–1.50. A larger fraction of the excess bond order resides in C1′–C2′ on the mutant enzyme, causing a substantial increase in the β-secondary isotope effect.

Conclusions. This work demonstrates the utility of transition-state analysis to understand the effects of mutations that affect catalysis. Analysis of structures by X-ray analysis gives a static picture of Michaelis-like complexes, but these are of limited use in the analysis of catalytic intermediates. Likewise, transition-state inhibitors may be of limited use for enzymes altered by site-directed mutagenesis, since altered catalytic-site structure may result in altered transition states. The mutant AMP nucleosidase shows no significant difference in its affinity for formycin 5′-phosphate when compared to the native enzyme (Leung & Schramm, 1981), while the differences in transition-state structures are easily measured by kinetic isotope effects and substrate specificity. The analysis of transition-state structure by kinetic isotope effects for enzymes before and after mutation provides direct information about catalytic structures at the transition state. The analysis of the mutant AMP nucleosidase demonstrates the usefulness of this approach.

REFERENCES

Bender, S. L., Widlanski, T., & Knowles, J. R. (1989) *Biochemistry 28*, 7560–7572.

Bennet, A. J., & Sinnott, M. L. (1986) *J. Am. Chem. Soc. 108*, 7287–7294.

Bigeleisen, J., & Wolfsberg, M. (1958) *Advances in Physical Chemistry I*, Interscience, New York.

Cleland, W. W. (1982) *Methods Enzymol. 87*, 625–641.

Cleland, W. W. (1987) *Bioorg. Chem. 15*, 283–302.

DeWolf, W. E., Jr., Fullin, F. A., & Schramm, V. L. (1979) *J. Biol. Chem. 254*, 10868–10875.

DeWolf, W. E., Jr., Emig, F. A., & Schramm, V. L. (1986) *Biochemistry 25*, 4132–4140.

Dreyfus, M., Dobin, G., Bensaude, O., & Dubuis, J. E. (1975) *J. Am. Chem. Soc. 97*, 2369–2376.

Elliott, A. C., Li, B. F., Morton, C. A. J., Pownall, J. D., Selwood, T., Sinnott, M. L., Souchard, I. J. L., & Stuart-Tilley, A. K. (1988) *J. Mol. Catal. 47*, 255–263.

Garrett, E. R., & Mehta, P. J. (1972) *J. Am. Chem. Soc. 94*, 8532–8541.

Giranda, V. L., Berman, H. M., & Schramm, V. L. (1988) *Biochemistry 27*, 5813–5818.

Gouaux, J. E., Krause, K. L., & Lipscomb, W. N. (1987) *Biochem. Biophys. Res. Commun. 142*, 893-897.
Hermes, J. D., Roeske, C. A., O'Leary, M. H., & Cleland, W. W. (1982) *Biochemistry 21*, 5106-5114.
Huskey, W. P. (1991) in *Origins and Interpretations of Heavy-Atom Isotope Effects* (Cook, P. F., Ed.) Chapter 2, CRC Press, Boca Raton, FL.
Kinoshita, Y., Ruble, J. R., & Jeffrey, G. A. (1981) *Carbohydr. Res. 92*, 1-7.
Kraut, J., & Jensen, L. H. (1963) *Acta Crystallogr. 16*, 79-88.
LaReau, R. D., Wan, W., & Anderson, V. (1989) *Biochemistry 28*, 3619-3624.
Leung, H. B., & Schramm, V. L. (1981) *J. Biol. Chem. 256*, 12823-12829.
Markham, G. D., Parkin, D. W., Mentch, F., & Schramm, V. L. (1987) *J. Biol. Chem. 262*, 5609-5615.
Melander, L., & Saunders, W. H., Jr. (1980) *Reaction Rates of Isotope Molecules*, pp 239-246, Wiley-Interscience, John Wiley and Sons, New York.
Mentch, F., Parkin, D. W., & Schramm, V. L. (1987) *Biochemistry 26*, 921-930.
Northrop, D. B. (1981) *Annu. Rev. Biochem. 50*, 103-131.
Parkin, D. W., & Schramm, V. L. (1984) *J. Biol. Chem. 259*, 9418-9425.
Parkin, D. W., & Schramm, V. L. (1987) *Biochemistry 26*, 913-920.
Parkin, D. W., Leung, H. B., & Schramm, V. L. (1984) *J. Biol. Chem. 259*, 9411-9417.
Rodgers, J., Femec, D. A., & Schowen, R. L. (1982) *J. Am. Chem. Soc. 104*, 3263-3268.
Scharschmidt, M., Fisher, M. A., & Cleland, W. W. (1984) *Biochemistry 23*, 5471-5478.
Schramm, V. L. (1974) *Anal. Biochem. 57*, 377-382.
Schuber, F., Travo, P., & Pascal, M. (1976) *Eur. J. Biochem. 69*, 593-602.
Sims, L. B., & Lewis, D. E. (1984) *Isot. Org. Chem. 6*, 161-259.
Sims, L. B., Burton, G. W., & Lewis, D. E. (1977) Quantum Chemistry Program Exchange No. 337, Indiana University, Bloomington, IN.
Sinnott, M. L. (1987) in *Enzyme Mechanisms* (Page, M. I., & Williams, A., Eds.) pp 259-297, Royal Society of Chemists, Burlington House, London.
Taylor, R., & Kennard, O. (1982) *J. Am. Chem. Soc. 104*, 3209-3212.
Wilson, E. B., Decius, J. C., & Cross, P. C. (1955) *Molecular Vibration*, McGraw-Hill Book Company, Inc., New York.
Wiórkiewicz-Kuczera, J., & Karplus, M. (1990) *J. Am. Chem. Soc. 112*, 5324-5340.
Zoltewicz, J. S., Clark, F. D., Sharpless, T. W., & Grabe, G. (1970) *J. Am. Chem. Soc. 92*, 1741-1750.

Structural and Functional Roles of Cysteine Residues of *Bacillus polymyxa* β-Amylase

Nobuyuki Uozumi, Tsukasa Matsuda, Norihiro Tsukagoshi,* and Shigezo Udaka

Department of Food Science and Technology, Faculty of Agriculture, Nagoya University, Chikusa-ku, Nagoya 464-01, Japan

Received October 3, 1990; Revised Manuscript Received January 2, 1991

ABSTRACT: *Bacillus polymyxa* β-amylase contains three cysteine residues at positions 83, 91, and 323, which can react with sulfhydryl reagents. To determine the role of cysteine residues in the catalytic reaction, cysteine residues were mutated to construct four mutant enzymes, C83S, C91V, C323S, and C-free. Wild-type and mutant forms of the enzyme were expressed in, and purified to homogeneity from, *Bacillus subtilis*. A disulfide bond between Cys^{83} and Cys^{91} was identified by isolation of tryptic peptides bearing a fluorescent label, IAEDANS, from wild-type and C91V enzymes followed by amino acid sequencing. Therefore, only Cys^{323} contains a free SH group. Replacement of cysteine residues with serine or valine residues resulted in a significant decrease in the k_{cat}/K_m value of the enzyme. C323S, containing no free SH group, however, retained a high specific activity, approximately 20% of the wild-type enzyme. None of the cysteine residues participate directly in the catalytic reaction.

The enzyme β-amylase (α-1,4-glucan maltohydrolase, EC 3.2.1.2) catalyzes the liberation of β-anomeric maltose from the nonreducing ends of α-1,4-glucan and is present in certain bacteria (Marshall, 1974; Murao et al., 1979; Shinke et al., 1974; Takasaki, 1976; Hyum & Zeikus, 1985) as well as in higher plants (Bernfeld, 1955; Kreis et al., 1987). Five genes encoding β-amylase have been cloned and sequenced from both prokaryotes and eukaryotes (Kawazu et al., 1987; Rhodes et al., 1987; Kitamoto et al., 1988; Toda et al., 1988; Kreis et al., 1987; Mikami et al., 1988). Three highly conserved sequences are recognized among them and are suggested to comprise the active site (Mikami et al., 1988). β-Amylases characterized to date are sensitive to various sulfhydryl-modifying reagents and are considered to contain an SH group essential for the activity (Murao et al., 1979; Hyum & Zeikus, 1985; Gertler & Birk, 1966; Spradlin & Thomas, 1970; Higashihara & Okada, 1974; Uehara & Mannen, 1979). The exact role of cysteinyl residues in the enzymatic action, however, remains uncertain, since the derivatization of the SH groups with alkylating reagents might inhibit the catalytic action only by steric hindrance at the active site (Mikami et al., 1980).

* To whom correspondence should be addressed.

0006-2960/91/0430-4594$02.50/0